Statistical Analysis of Wind and Solar Energy Potential in Tehran

Majid Vafaeipour*‡, Mohammad H. Valizadeh**, Omid Rahbari*, Mahsa Keshavarz Eshkalag***

* Department of Energy Systems Engineering, Faculty of Engineering, Islamic Azad University-South Tehran Branch, Iran

** Iran University of Science and Technology, School of Electrical Engineering, Iran

*** Faculty of Management and Accounting, Islamic Azad University-South Tehran Branch, Iran

(St_M_Vafaeipour@azad.ac.ir, Valizadeh.mh@gmail.com, St_O_Rahbari@azad.ac.ir, Mahsa.Keshavarz90@gmail.com)

‡Corresponding Author; Department of Energy Systems Engineering, Faculty of Engineering, Islamic Azad University-South Tehran Branch, Tehran, Iran, Majid.Vafaeipour@gmail.com

Received: 03.01.2014 Accepted: 26.03.2014

Abstract- Knowing the potential of wind and solar energy resources is vital to determine significant information of sizing, installing and implementation of renewable energy systems in a given region. The present study identifies wind and solar energy properties of a studied area located in Tehran, Iran, using input meteorological data measured for one year period provided by the Iran Renewable Energy Organization from a ground station, Letman Jungle. Many prior studies are limited in using average wind speed without classification of the resource. However, the present paper adopts the random fluctuations of wind speed data for classification purpose. Furthermore, it utilizes a temperature-based method to estimate solar energy potential of the region. In this regard, daily and monthly average amounts of global solar irradiation on horizontal surface are calculated all around a year. Regarding wind energy resource properties, the most probable wind speed and its direction, the velocity which carries the maximum energy, the average wind power density, and the wind energy density of the region are all calculated and discussed. Investigation of the results indicates harnessing solar energy would be more favourable for the studied region.

Keywords- Energy resource, Wind energy potential, Solar energy potential, Wind power density, Weibull distribution, Temperature-based method

1. Introduction

The rapid rising amount of energy consumption as a result of modernity besides industrial and agricultural development has been a main issue of energy discussions recently. Based on current reserves and consumption rate of fossil resources, the world will sustain 122 years for coal, 42 years for oil and 60 years for natural gas [1]. Global warming, depletion of fossil resources, population growth and environmental awareness plus increasing energy demands are of the vital factors to consider utilization clean energy much promising [2, 3]. Figs. 1-2, provided by the World Renewables Report 2011, illustrate the growth of employing wind and solar energy in recent years. During 2010, the new capacity added for wind power has reached by 39 GW, and almost 17 GW of photovoltaic capacity was added globally in 2010 comparing to 7.3 GW in 2009 [4].

Estimating potential of these resources has been the interested field of a number of researchers throughout the literature. Kamau et al. [5] employed 6 years of wind data to estimate wind energy potential and found Marsabit as a suitable location for stand-alone and grid connected power generation. To estimate wind mean power density, which is of the preliminary information of installing feasible wind farms, statistical investigations have been performed in Hong Kong, UK, South Africa and Eastern Mediterranean [6-9]. In other studies, Rumachandra et al. [10] and Sliz-Szkliniarz et al. [11] utilized GIS-based methods to investigate wind energy potential in India and Germany, respectively. In a comparison thorough 7 numerical methods, Paulo Alexandre Costa Rocha reached smaller errors in fitting Weibull distribution curves via employing numerical approaches based on mathematical iterations for defining shape and scale parameters [12].

Different TB methods has been developed and modified through the history of solar radiation research. In this regard, Table 1 presents an overview where most of the proposed methods are derived from the Hargreaves model. The difference between TB models with same parameters is due to their various empirical coefficients and the calculation way of their constituting parameters.

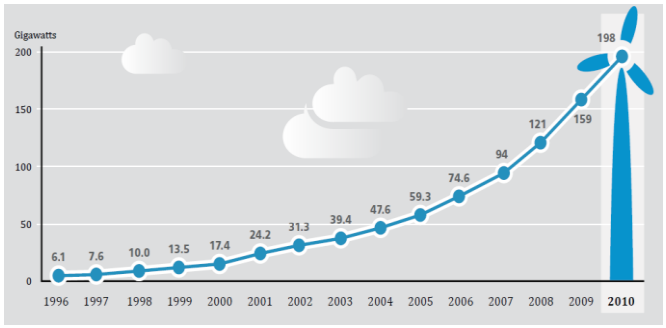

Fig. 1. Wind power-Existing world capacity (1996-2010) [4]

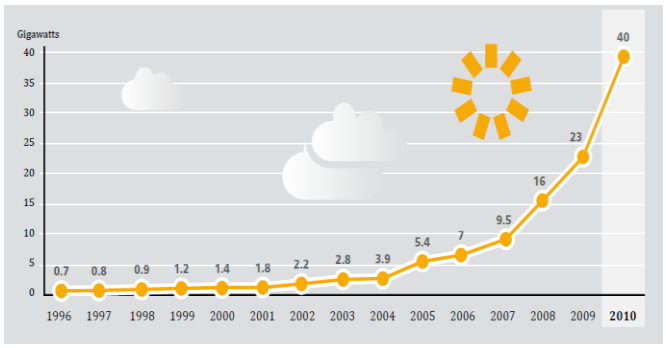

Fig. 2. Solar PV-Existing world capacity (1996-2010) [4]

In the present study, the renewable energy potential of wind and solar energy resources and their relevant properties are evaluated via using input meteorological data measured for one year period from the studied ground station, Letman Jungle, located in the west of Tehran city. For this, a TB method is used for estimation of global solar irradiation on a horizontal surface, and the wind energy properties of the region are obtained via utilizing a statistical approach.

2. Analytic Methods

2.1. Wind Analysis

The power per unit area transported by a fluid system is related to the cube of the fluid speed [5]:

$$P(v) = \frac{1}{2}\rho A v^3 \quad (1)$$

In the above equation, power of the wind that flows at speed v through a blade sweep area A (m^2) and ρ density can be calculated. ρ equals 1.225 kg/m^3 which is the standard air density at the sea level with mean ambient temperature of 15 $^{\circ}C$ and 1 atmospheric pressure. In order to decide which statistical distribution or probability density function (PDF) fits to wind speed data: a) a null hypothesis is set, b) test statistic is obtained, and c) considering decision rule (of the null hypothesis) decision regarding acceptance or rejection of the fitness alternate PDF is made. The Null hypothesis is considered as: H0: Estimated PDF of wind speed data set. Decision rules for acceptation or rejection of the mentioned hypothesis are given: if the calculated p-value based on applying a proper goodness of fit test is greater than the significant level (i.e. 0.05) accept H0; otherwise reject it [18].

Table 1. Temperature-based models

Model (Authors et al.)	Year	Indicators
Almorox	2011	H_0 , T_{max} , T_{min}
Duat	2011	H_0 , T_{max} , T_{min}
Mahmood	2002	H_0 , T_{max} , T_{min} , ϕ , DOY, LDY
Annandale	2002	H_0 , T_{max} , T_{min} , Z
Winslow	2001	H_0 , T_{max} , T_{min} , T_{mean} , H_{day}, ϕ
Goodin	1999	H_0 , T_{max} , T_{min}
Donatelli	1998	H_0 , T_{max} , T_{min}
Allen	1997	H_0 , T_{max} , T_{min}
Bristow	1984	H_0 , T_{max} , T_{min}
Hargreaves	1982	T_{max} , T_{min}

H_0 extraterrestrial solar radiation, T_{max} daily maximum air temperature, T_{min} daily minimum air temperature, T_{mean} mean annual temperature, ϕ latitude, DOY day of year, LDY longest DOY, H_{day} half-day length

fitness alternate PDF is made. The Null hypothesis is considered as: H0: Estimated PDF of wind speed data set. Decision rules for acceptation or rejection of the mentioned hypothesis are given: if the calculated p-value based on applying a proper goodness of fit test is greater than the significant level (i.e. 0.05) accept H0; otherwise reject it [18].

In many cases among all density functions, the Weibull distribution could act as an appropriate fitness alternative for wind speed PDF [19]. Weibull function has flexibility and simplicity and provides a logical fit to experimental data when applying to wind data [20]. Eq. 2 represents the Weibull probability function with shape and scale parameters of k and c respectively:

$$f(v) = \frac{k}{c}\left(\frac{v}{c}\right)^{k-1}\exp\left[-\left(\frac{v}{c}\right)^{k}\right] \quad (2)$$

To indicate the fraction of time the wind speed is equal or lower than speed v, the cumulative distribution function (CDF) of velocity is:

$$F(v) = 1-\exp\left[-\left(\frac{v}{c}\right)^{k}\right] \quad (3)$$

The average wind velocity and its variance of wind can be calculated using the measured data via Eqs. 4-5.

$$\bar{v} = \frac{1}{n}\sum_{i=1}^{n} v_i \quad (4)$$

$$\sigma^2 = \frac{1}{n-1}\sum_{i=1}^{n}(v_i - \bar{v})^2 \quad (5)$$

As follows in Eq. 6, the Weibull function parameters, k (shape factor) and c (scale factor), can be approximated:

$$k = (\frac{\sigma}{\bar{v}})^{-1.086} \quad (1 \le k \le 10) \tag{6}$$

$$c = \frac{\bar{v}}{\Gamma(1+\frac{1}{k})} \tag{7}$$

where the gamma function (Γ) can be obtained via utilizing Stirling approximation as follows:

$$\Gamma(x) = \int_0^\infty e^{-u} u^{x-1} du \tag{8}$$

The average power density based on the Weibull PDF is given as:

$$\frac{P}{A} = \int_0^\infty \frac{1}{2}\rho v^3 f(v) dv = \frac{1}{2}\rho c^3 \Gamma(\frac{k+3}{k}) \tag{9}$$

Knowing wind power density (*P/A*), wind energy density for a favorable duration of *T*, can be obtained via Eq. 10.

$$\frac{E}{A} = \frac{1}{2}\rho c^3 \Gamma(\frac{k+3}{k})T \tag{10}$$

After the scale and shape parameters of Weibull function are yielded, the most probable wind speed (V_{mp}) and the wind speed which carries the maximum energy $V_{max,E}$ can be calculated as represented in the following Eqs.:

$$V_{mp} = c(1-\frac{1}{k})^{\frac{1}{k}} \tag{11}$$

$$V_{\max,E} = c(1+\frac{2}{k})^{\frac{1}{k}} \tag{12}$$

2.2. Solar Analysis

Using the ambient temperature difference, Hargreaves and Samani [21] suggested Eq. 13 to estimate global solar irradiation R_s.

$$R_s = K_r (T_{\max} - T_{\min})^{0.5} R_a \tag{13}$$

In the above-mentioned Eq., K_r is an empirical coefficient and R_a is the extraterrestrial radiation. K_r is an unit-less coefficient which varies for different atmospheric conditions and can be taken equal to 0.17 for arid and semi-arid climates, respectively. It also presented by Hargreaves equal to 0.16 and 0.19 for interior and coastal regions, respectively [21]. Later on, Allen [22] introduced a correction factor for K_r which can be seen in Eq. 14.

$$K_r = K_{ra}(\frac{p}{p_0})^{0.5} \tag{14}$$

where p and p_0 are the mean atmospheric pressure of the site and the mean atmospheric pressure at sea level, 101.3 kPa, respectively. Mean pressure of the site, can be either considered using the measured data of the site or the estimated values according to Burman equation as it follows [23]. For the purpose of the current study, measured mean pressure data is employed.

$$P = P_o(\frac{293 - 0.0065Z}{293})^{5.26} \tag{15}$$

where *Z* would be the height in m. In Eq. 14, the value of empirical coefficient K_{ra} equals 0.17 and 0.2, suggested by Allen for interior and coastal regions respectively [22]. It is notable that Eq. 14 performs inefficient for elevations higher than 1500 meters [15] in contrast with the elevation of the studied region. Another way to calculate K_{ra} is to use Samani's modified form via using maximum and minimum ambient temperature differences as given in Eq. 16:

$$K_r = 0.00185(T_{\max} - T_{\min})^2 - 0.0433(T_{\max} - T_{\min}) + 0.4023 \tag{16}$$

$$\delta = 23.45 sin[\frac{360}{365}(284 + n)] \tag{17}$$

In Eq. 17, the sun declination angle (δ), is the angle between the joining line of the centers of the sun and the earth and its projection on the equatorial plane, and depends on the nth day of the year. Introducing the hour angle (ω) which the earth must rotate to take meridian plane under the sun, the sunset hour angle (ω_s) will be as follows:

$$\omega_s = cos^{-1}(-Tan\phi Tan\delta) \tag{18}$$

where ϕ is latitude of the location. As follows, Eq. 19 defines the angle between the sun's ray and perpendicular line to the horizontal plane called Zenith (Polar) angle.

$$cos\theta_z = cos(\phi)cos(\delta)sin(\omega_s) + \omega_s sin(\phi)sin(\delta) \tag{19}$$

The solar radiation outside the atmosphere on a horizontal plane (I_o) for *n*th day of the year, considering the I_{SC} (solar constant) which is defined equal to 1367 $\frac{w}{m^2}$ by the world meteorological organization (WMO) standard, is given in Eq. 20 [16, 17].

$$I_o = I_{SC}[1 + 0.033cos(\frac{360n}{365})]cos\theta_z \tag{20}$$

To calculate the integrated daily extraterrestrial radiation on a horizontal surface (R_a), Eq. 21 can be employed.

$$R_a = \frac{24 \times 3600}{\pi} I_0 \tag{21}$$

3. Area and Using Data

Tehran, a populated city and the capital of Iran is located at altitude of 1190.8 m from the sea level. The utilized data of the study is measured for one year period by the Iran Renewable Energy Organization from a ground station, Letman Jungle, located in the west of Tehran. The input utilized data include maximum, minimum and average of the daily ambient temperature, and the pressure to evaluate the status of global solar irradiation on horizontal surface. Also, wind velocity data with 1 hour intervals are utilized to obtain wind energy properties of the region. In this regards, monthly maximum, minimum and average atmospheric pressures and ambient temperatures are shown in Table 2 via using the measured daily data. Also, Figs. 3-4 illustrate the changes regarding monthly mean wind velocity and monthly mean ambient temperature, respectively. From the average of daily measured data, it can be seen that Tehran experiences its coldest and hottest months in January (-4 $^{\circ}C$) and July (42 $^{\circ}C$) respectively.

Table 2. The monthly maximum, minimum ambient temperature and average atmospheric pressure of the collected data

	Max Temp	Min Temp	Mean P
Jan	13	-4	101.85
Feb	14	-4	101.25
Mar	23	-2	101.73
Apr	23	7	101.43
May	36	14	101.45
Jun	39	19	100.94
Jul	42	24	101.06
Aug	40	15	101.1
Sep	34	17	101.43
Oct	31	6	101.81
Nov	18	-1	101.9
Dec	13	-1	102.28

Maximum of the mean wind speed occurs at March (5.20 m/s) which may result highest wind potential in this month depending on Weibull function parameters. Yearly average of wind speed equals 4.09 m/s and the monthly mean wind speed exhibits its biggest variation from February to March and April to May.

To handle the uncertainties caused by the discontinuous nature of wind velocity, the fitted PDF over histogram of the measured wind data of the region is plotted in Fig. 5. As can be seen, the PDF follows the Weibull function's general pattern appropriately. Also, the plot for Weibull parametric cumulative distribution is shown in Fig. 6 which indicates the probability where wind speed is equal or lower than speed *v*. The monthly calculated values of V_{mp} and $V_{max,E}$ are plotted in Fig. 7 via using the shape and scale parameters of the Weibull function.

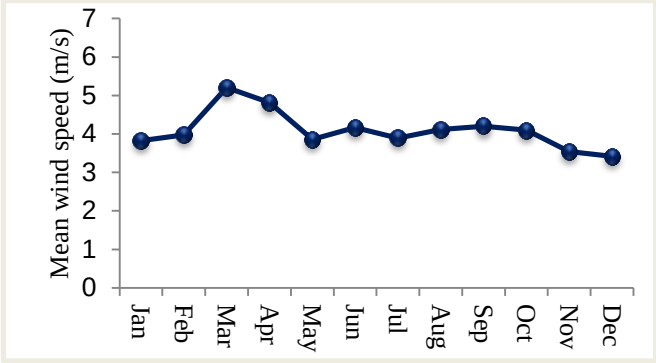

Fig. 3. The monthly mean wind speed changes of the collected data

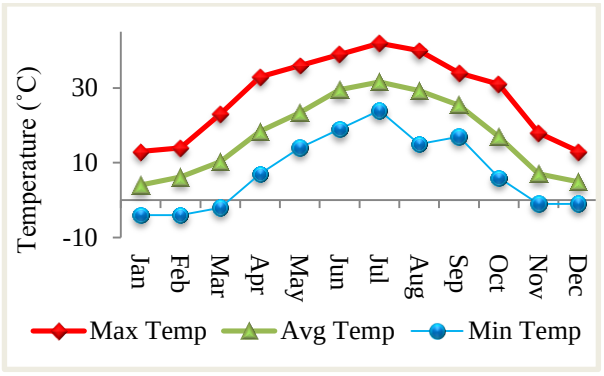

Fig. 4. The temperature changes of the collected data

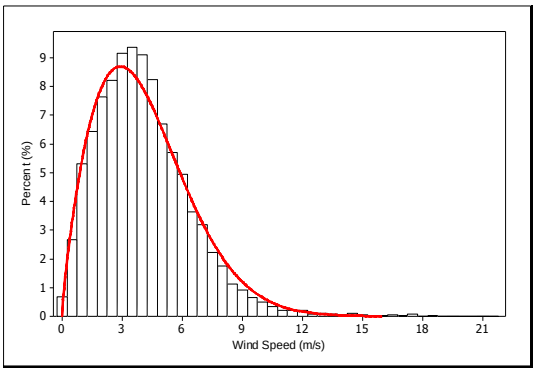

Fig. 5. Weibull pdf curve and the collected wind velocity data histogram

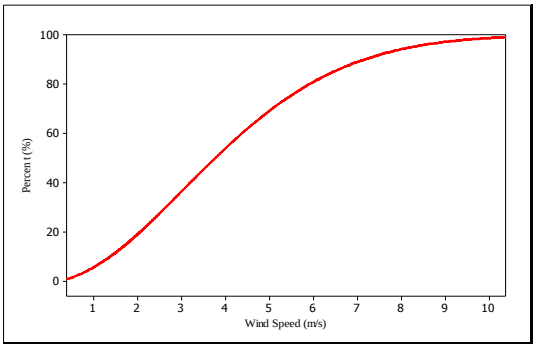

Fig. 6. The cumulative distribution function of the collected wind velocity data

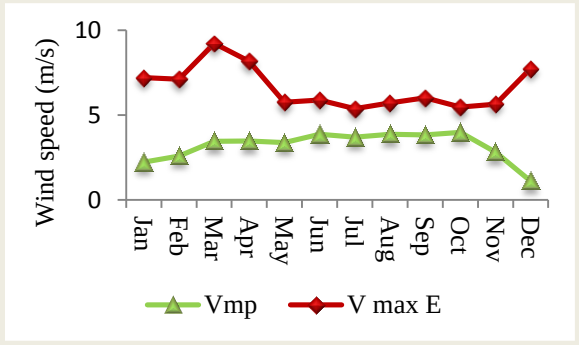

Fig. 7. The monthly mean V_{mp} and $V_{max,E}$

4. Results and Discussion

Via using the mentioned equations of the solar analysis section, Fig. 8-9 illustrate the yielded status of monthly and daily global solar irradiation on horizontal surface (R_s) in 2011 for the studied region. As can be seen in Fig. 9, lower values of R_s are obtained in colder seasons (October to March), which is logical due to lower difference of temperatures according to Fig. 4 and Hargreaves Equation. Also due to the same reason; although the highest and the lowest ambient temperatures occur in July and January, the highest and the lowest average of the received global solar radiation on horizontal surface occur at June (7.46 kWh/m^2 /day) and December (2.46 kWh/m^2 /day), respectively. The amount of the total annual received global solar radiation on horizontal surface for the studied region resulted in 1.85 MWh/m^2/year for 2011. The high solar potential of the region makes it acceptable to invest more on solar energy systems projects.

As illustrated in Fig. 7, the maximum values of V_{mp} and $V_{max,E}$ may not occur at same months and the possibility of blowing lower but more continual (more energy is being carried) wind can be a logical reason of this issue. As can be seen, the most probable wind speed obtains its highest value (3.86 m/s) in June in comparing to other months. However, maximum value of the wind which carries the maximum energy occurs in March (9.21 m/s). Table 3 presents the results of mean velocity, standard deviation, shape and scale parameters of Weibull function throughout the besides the calculated wind power density (W/m^2) and the energy density (kWh/m^2/year).

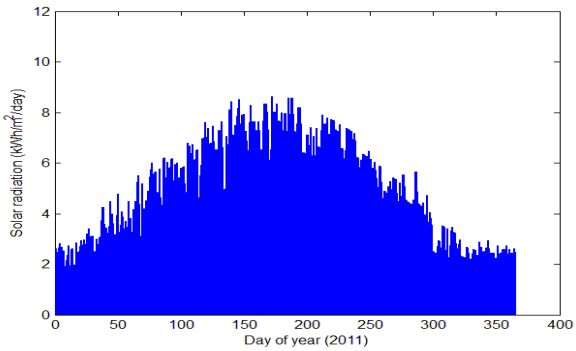

Fig. 8. Estimated daily global solar irradiation on horizontal surface

The highest value of wind power density equals 202.03 W/m^2 and its lowest value is 50.91 W/m^2, occurred in March and July respectively. The wind energy density ranges between 445.83-1769.12 kWh/m^2/year in Tehran.

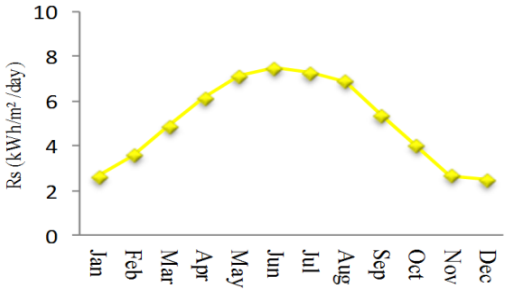

Fig. 9. Estimated monthly daily average global solar irradiation on horizontal surface

Table 3. Calculated monthly wind properties

Month	Σ	Mean V	K	C	P/A	E/A
Jan	2.53	3.82	1.57	4.26	91.53	801.47
Feb	2.47	3.98	1.68	4.45	92.59	810.74
Mar	3.19	5.20	1.70	5.83	202.03	1769.12
Apr	2.79	4.81	1.81	5.41	143.63	1257.70
May	1.81	3.86	2.28	4.35	58.04	508.23
Jun	1.76	4.17	2.55	4.69	65.30	571.81
Jul	1.56	3.89	2.71	4.38	50.91	445.83
Aug	1.68	4.11	2.65	4.63	61.37	537.42
Sep	1.83	4.20	2.47	4.74	69.91	612.13
Oct	1.51	4.10	2.96	4.59	59.45	520.54
Nov	1.87	3.54	2.00	3.99	53.66	469.84
Dec	2.73	3.42	1.28	3.69	91.05	797.31

The European Wind Energy Association (EWEA) [24] has categorized wind characteristics as follows in Table 4 and another wind density classification for 10 m height is presented in Table 5 via considering Min and Max of wind speed as well as wind power density [25].

Table 4. Wind categories based on EWEA classification

Category	Wind Characteristics
Fairly good	6.5 (m/s) ≈ (300-400 W/m^2)
Good	7.5 (m/s) ≈ (500-600 W/m^2)
Very Good	8.5 (m/s) ≈ (700-800 W/m^2)

Table 5. Wind power classifications (10 m) [25]

Wind class	Min wind speed (m/s)	Max wind speed (m/s)	Min wind power density (W/m^2)	Min wind power density (W/m^2)
1	0	4.4	0	100
2	4.4	5.1	100	150
3	5.1	5.6	150	200
4	5.6	6.0	200	250
5	6.0	6.4	250	300
6	6.4	7.0	300	400
7	7.0	9.4	400	1000

In Fig. 10, measured wind data of the studied site is classified via considering the standards mentioned in Table 5. As can be seen, almost 60% of the existed wind in Tehran is classified in class 1. According to Table 5, Table 4 and the calculated mean wind power density in Table 3, Tehran is not suitable for installing large scale wind turbines. Tehran is a city surrounded by mountains and this would be a cause of low wind potential besides meteorological parameters which result in air convections. However, small scale wind turbines can be employed to supply electricity to off-grid systems such as chargers, electric fans, lightening and mechanical applications in agricultural activities like water pumping. In order to analyze wind energy properly, determining wind

direction accompanied by its other properties is a significant issue in wind energy systems research. To illustrate wind direction accompanied by its velocity, wind roses which are polar diagrams are helpful tools in wind energy investigations. Based on wind direction data which is measured clock wise in degrees, wind frequencies (%) are plotted in a polar diagram with respect to the cardinal point from which the wind blows. The wind rose is divided to 16 sectors and each of them covers an arc of 22.5°. Fig. 11 illustrates the wind rose of the studied region, and Fig. 12 plots it on the location where the utilized wind data of the study was provided from. From Fig. 11 it can be seen that the most probable wind direction of the region is in the quadrant which correspond to the south east.

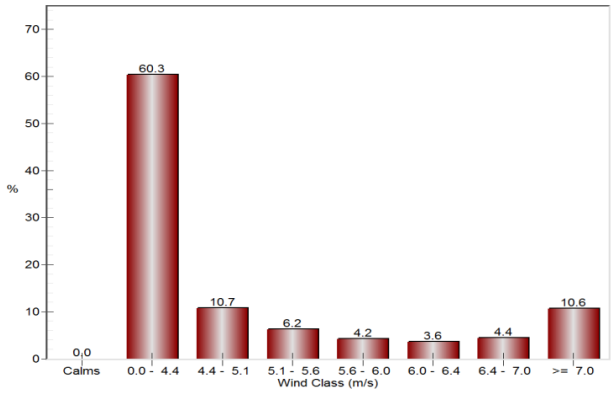

Fig. 10. Classification of existed wind velocities in Tehran based on Table 5

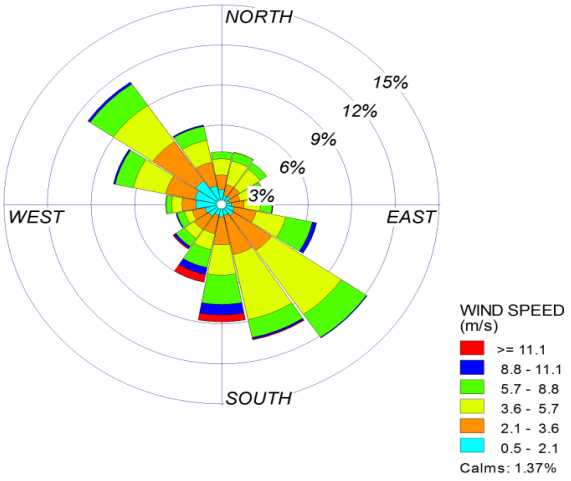

Fig. 11. Wind rose of the studied region

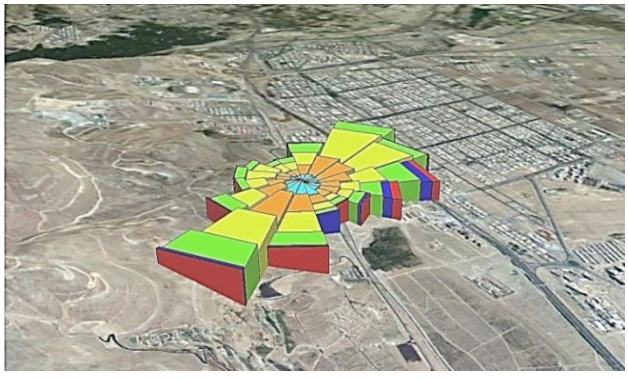

Fig. 12. 3D Wind Rose of the studied region

5. Conclusions

Wind and solar energy are renewable and environmental-friendly. They are alternate clean energy sources associated to the fossil fuels that contaminate our atmosphere. Via using the available measured data provided by a ground meteorological station in Tehran, Iran, this study evaluated the status of solar and wind energy potential. The daily and monthly global solar irradiation on horizontal surface and various wind energy properties were assessed using a temperature-based method and Weibull distribution function, respectively. To investigate the most probable direction of the wind, wind direction and velocity data were employed to plot the 2D and 3D wind roses of the region. The sum of received annual global solar radiation on horizontal surface yielded 1.85 MWh/m^2/year for 2011. The highest and the lowest ambient temperatures occurred in July and January but the highest and the lowest average of global solar irradiation were estimated in June (7.46 kWh/m^2 /day) and December (2.46 kWh/m^2/day), respectively. Wind analysis indicated that the region experiences its maximum average velocity in March, April and February. The yearly mean wind speed ranged between 3.42-5.2 m/s values related to December and March. The yearly average of wind speed was equal to 4.09 m/s and the biggest variations of monthly mean wind speed were observed from February to March and April to May. The most probable wind speed direction was at the quadrant which corresponded to the south east. The yearly average wind power density ranged between 50.91 and 202.03 W/m^2 which is not desirable for using large scale wind turbines but it will be sufficient for using small scale turbines for small size non-grid electricity generation. Although the investigations demonstrate higher solar energy potential in comparison with wind energy density in Tehran, it is notable that for the months with lower irradiation such as January, February, March and April, the wind energy density reaches to its highest values. This can support probable feasibility of employing reliable PV-wind hybrid energy systems in the region to be evaluated. Also, economic programming and developing policies to employ the investigated resources in an optimized way merit further investigations via considering the renewable energy characteristics of the region.

References

[1] M. S. H. Lipu, M. S. Uddin, and M. A. R. Miah, "A Feasibility Study of Solar-Wind-Diesel Hybrid System in Rural and Remote Areas of Bangladesh," International Journal of Renewable Energy Research (IJRER), vol. 3, pp. 892-900, 2013.

[2] F. Fazelpour, M. Vafaeipour, O. Rahbari, and R. Shirmohammadi, "Considerable parameters of using PV

cells for solar-powered aircrafts," Renewable and Sustainable Energy Reviews, vol. 22, pp. 81-91, 2013.

[3] M. Vafaeipour, O. Rahbari, M. A. Rosen, F. Fazelpour, and P. Ansarirad, "An artificial neural network approach to predict wind velocity time-series in Tehran," in The 5th International Congress of Energy and Environment Engineering and Management, Lisbon, 2013.

[4] "REN21. Renewables Global Status Report," 2011.

[5] J. N. Kamau, R. Kinyua, and J. K. Gathua, "6 years of wind data for Marsabit, Kenya average over 14m/s at 100m hub height; An analysis of the wind energy potential," Renewable Energy, vol. 35, pp. 1298-1302, 2010.

[6] B. Safari and J. Gasore, "A statistical investigation of wind characteristics and wind energy potential based on the Weibull and Rayleigh models in Rwanda," Renewable Energy, vol. 35, pp. 2874-2880, 2010.

[7] I. Y. F. Lun and J. C. Lam, "A study of Weibull parameters using long-term wind observations," Renewable Energy, vol. 20, pp. 145-153, 2000.

[8] D. Weisser, "A wind energy analysis of Grenada: an estimation using the 'Weibull' density function," Renewable Energy, vol. 28, pp. 1803-1812, 2003.

[9] S. A. Akdağ, H. S. Bagiorgas, and G. Mihalakakou, "Use of two-component Weibull mixtures in the analysis of wind speed in the Eastern Mediterranean," Applied Energy, vol. 87, pp. 2566-2573, 2010.

[10] T. V. Ramachandra and B. V. Shruthi, "Wind energy potential mapping in Karnataka, India, using GIS," Energy Conversion and Management, vol. 46, pp. 1561-1578, 2005.

[11] B. Sliz-Szkliniarz and J. Vogt, "GIS-based approach for the evaluation of wind energy potential: A case study for the Kujawsko–Pomorskie Voivodeship," Renewable and Sustainable Energy Reviews, vol. 15, pp. 1696-1707, 2011.

[12] P. A. Costa Rocha, R. C. de Sousa, C. F. de Andrade, and M. E. V. da Silva, "Comparison of seven numerical methods for determining Weibull parameters for wind energy generation in the northeast region of Brazil," Applied Energy, vol. 89, pp. 395-400, 2012.

[13] F. Fazelpour, M. Vafaeipour, O. Rahbari, and M. A. Rosen, "Intelligent optimization to integrate a plug-in hybrid electric vehicle smart parking lot with renewable energy resources and enhance grid characteristics," Energy Conversion and Management, vol. 77, pp. 250-261, 2014.

[14] F. Fazelpour, M. Vafaeipour, O. Rahbari, and M. A. Rosen, "Intelligent optimization of charge allocation for plug-in hybrid electric vehicles utilizing renewable energy considering grid characteristics," in Smart Energy Grid Engineering (SEGE), 2013 IEEE International Conference on, 2013, pp. 1-8.

[15] R. G. Allen, "Self-calibrating method for estimating solar radiation from air temperature. ," Hydrology Engineering vol. 2, pp. 56-67, 1997.

[16] A. David and N. R. Ngwa, "Global Solar Radiation of some regions of Cameroon using the linear Angstrom and non-linear polynomial relations (Part I) model development," International Journal of Renewable Energy Research (IJRER), vol. 3, pp. 984-992, 2013.

[17] F. Fazelpourl, M. Vafaeipour, O. Rahbaril, and M. H. Valizadehz, "Assessment of solar radiation potential for different cities in Iran using a temperature-based method," Sustainability in Energy and Buildings: Proceedings of the 4th International Conference in Sustainability in Energy and Buildings (SEB12), vol. 22, pp. 199-208, 2013.

[18] S. Raissi and M. Kariminasab, Computer Aided Mathematical Modeling vol. 1. Tehran: Islamic Azad University-South Tehran Branch, 2006.

[19] O. Rahbari, M. Vafaeipour, F. Fazelpour, M. Feidt, and M. A. Rosen, "Towards realistic designs of wind farm layouts: Application of a novel placement selector approach," Energy Conversion and Management, vol. 81, pp. 242-254, 2014.

[20] M. Vafaeipour, O. Rahbari, M. A. Rosen, Fazelpour, Farivar, and S. M. Heibati, "Optimal sizing of a hybrid energy system for a semi-arid climate using an evolutionary algorithm," International Journal of Renewable Energy Technology, 2013.

[21] G. H. Hargreaves and Z. A. Samani, "Reference crop evapotranspiration From ambient air temperature," presented at the International Irrigation Center, winter meeting, American society of agricultural engineers, UT, USA, 1985.

[22] R. G. Allen, "Evaluation of procedures for estimating mean monthly solar radiation from air temperature," presented at the Rep, (FAO) Rome, Italy, 1995.

[23] R. D. Burman, M. Jensen, and R. G. Allen, "Thermodynamic factors in evapotranspiration," in Irrigation and Drainage Specialty Conference, ASCE, Portland, Ore, 1987 pp. 28-30.

[24] A. Garrad, "Wind energy in Europe: a plan of action, summary report of wind energy in Europe—time for action " The European Wind Energy Association1991.

[25] A. Mostafaeipour, A. Sedaghat, A. A. Dehghan-Niri, and V. Kalantar, "Wind energy feasibility study for city of Shahrbabak in Iran," Renewable and Sustainable Energy Reviews, vol. 15, pp. 2545-2556, 2011.